Biol Invasions
DOI 10.1007/s10530-015-0893-4

ORIGINAL PAPER

An age-structured bio-economic model of invasive species management: insights and strategies for optimal control

İ. Esra Büyüktahtakın · Eyyüb Y. Kıbış · Halil I. Cobuloglu · Gregory R. Houseman · J. Tanner Lampe

Received: 14 October 2014 / Accepted: 31 March 2015

Abstract Controlling invasive species is a highly complex problem defined by the biological characteristics of the organisms, the landscape context, and a management objective of minimizing invasion damages given limited financial resources. While bio-economic optimization models provide a promising approach for invasive species control, current spatio-temporal optimization models omit key ecological details such as age structures—which could be essential to predict how populations grow and spread spatially over time and determine the most effective control strategies. We develop a novel age-structured optimization model as a spatial-dynamic decision framework for controlling invasive species. In particular, we propose a new carrying capacity sub-model, which allows us to take into account the biological competition among different age classes within the population. The potential use of the model is demonstrated on controlling the invasion of sericea (*Lespedeza cuneata*), a perennial legume threatening native grasslands in the Great Plains. The results show that incorporating age-structure into the model captures important biological characteristics of the species and leads to unexpected results such as multi-logistic population growth with multiple, sequential, and overlapping phases of logistic form. These new findings can contribute to understanding time-lags and invasion growth dynamics. Additionally, given budget constraints, utilizing control measures every 2–3 years is found to be more effective than yearly control because of the time to reproductive maturity. Results of the bio-economic optimization approach provide both ecological and economic insights into the control of invasive species. Furthermore, while the proposed model is specific enough to capture biological realism, it also has the potential to be generalized to a wide range of invasive plant and animal species under various management scenarios in order to identify the most efficient control strategies for managing invasive species.

Keywords Age-structure · Biological invasion control · Invasive species · Multi-logistic growth · Non-linear optimization · Resource allocation · Seed bank · Sericea (*Lespedeza cuneata L.*) · Spatio-temporal model · Weed management

Electronic supplementary material The online version of this article (doi:10.1007/s10530-015-0893-4) contains supplementary material, which is available to authorized users.

İ. E. Büyüktahtakın (✉) · E. Y. Kıbış · H. I. Cobuloglu · J. T. Lampe
Department of Industrial and Manufacturing Engineering, Wichita State University, 1845 N. Fairmount, Wichita, KS 67260-0035, USA
e-mail: esra.b@wichita.edu

G. R. Houseman
Department of Biological Sciences, Wichita State University, 1845 N. Fairmount, Wichita, KS 67260-0026, USA

Journal : **Medium 10530**	Dispatch : **9-4-2015**	Pages : **19**
Article No. : **893**	☐ LE	☐ TYPESET
MS Code : **BINV-D-14-00515**	☑ CP	☑ DISK

Introduction

Controlling species invasions at the landscape scale is a highly complex problem. First, the rates of spread and impact on native communities are critically dependent on life span, growth rates, dormant stages, and dispersal, which may not be captured by simple population growth functions (Gurevitch et al. 2011). Second, landscapes are heterogeneous, and invasions often do not follow simple patterns of spread from a given introduction point (Schreiber and Lloyd-Smith 2009; With 2002). Third, available resources (time and money) are almost always limited. When these factors are combined, intuitively determining the most efficacious control strategy quickly becomes intractable. For this reason, optimization models of invasion control that explicitly incorporate limited budgets can be useful decision tools to analyze the potential consequences of different control strategies (for a detailed review of these studies, see, e.g., Olson 2006; Epanchin-Niell and Hastings 2010; Billionnet 2013).

Although bio-economic optimization models for invasion control are not new (Clark 1990), advances in optimization and computational power offer new opportunities to incorporate much greater ecological realism than previously possible. Several optimization models demonstrate the importance of spatio-temporal processes when controlling invaders (Bhat et al. 1993; Hof 1998; Hof and Bevers 2002; Albers et al. 2010; Blackwood et al. 2010; Kaiser and Burnett 2010; Büyüktahtakın et al. 2011; Epanchin-Niell and Wilen 2012; Kovacs et al. 2014). While the progress in spatial–temporal modeling is encouraging, the real potential for such models remains under-utilized, because those models omit key ecological details such as age structures—which could be essential to forecast how populations grow spatially over time and determine the most effective control strategies. In this paper, we present a novel age-structured optimization model as a spatial-dynamic decision framework for controlling invasive species, and demonstrate the potential use of the model for controlling the invasion of sericea (*Lespedeza cuneata*), a perennial legume threatening native grasslands in the Great Plains. In particular, we develop a new carrying capacity sub-model, which allows us to take into account the biological competition among different age classes within the population. The results demonstrate that incorporating age-structure into the model captures important biological characteristics of the species and lead to unexpected results such as multi-logistic population growth (see Appendix S1). These new findings can contribute to understanding time-lags and invasion growth dynamics thus provide new insight into controlling invaders.

We include the age structure of invasive species in the model because reproduction and survival vary with plant age. The simplest age-structured model is the Leslie Model (Leslie 1945), where the population is divided into discrete age classes. Structured models include age-, weight-, stage-, and size-structured models (see, e.g., Getz and Haight 1989; Caswell 2001; Taylor and Hastings 2004). Among all these possible structuring alternatives, we consider an age-structured model of the invasive species control because, for many species, reproduction and survival rate differ with age (see, e.g., Woods et al. 2009). The seed stage is particularly important because seeds can either germinate quickly or form a long-term seed bank, which builds a reservoir of potential propagules that can increase future weed infestations (Wu 2001). Our model is unusual in that it accounts for density, frequency, age, dispersal, and seed bank dynamics of the invaders simultaneously in a spatio-temporal landscape to determine the optimal placement and timing of invasion control.

Here, population growth is formulated considering the germination of seeds from the seed bank and dispersed seeds, as opposed to the use of a logistic growth function, which is a central assumption in previous invasion control models. The seed bank-based linear growth model contributes to the optimization of spatio-temporal population dynamic models by significantly improving its solvability compared to non-linear logistic growth counterparts while maintaining much greater biological complexity than other logistic or constant growth models. Furthermore, the model incorporates different seed production and loss rates by dividing the population into different age classes, and it tracks the growth of each age class over a multi-period time horizon. Incorporating seed bank growth and age structure into the model provides insight into population growth patterns, which is found to be more complex than the simple logistic growth (Stone 1980) and has important implications for control strategies.

Journal : Medium 10530 | Dispatch : 9-4-2015 | Pages : 19
Article No. : 893 | ☐ LE | ☐ TYPESET
MS Code : BINV-D-14-00515 | ☑ CP | ☑ DISK

We also consider uncertainty in our deterministic model by performing sensitivity analysis of different uncertain parameters such as budget, treatment efficacy, and dispersal rate. In addition, we examine model solutions in order to provide the minimum necessary level of resources (labor and budget) that could efficiently control the invader under different initial population distribution scenarios. Finally, we evaluate the effectiveness of different treatment frequency strategies for controlling invasion damages.

Materials and methods

Bio-economic model of invasive species control

The bio-economic model is formulated as follows: Let T denote the time horizon, and let $t \in [0, T]$ be any year of the planning horizon. The area consists of rectangular cells with I rows and J columns. Any cell can be characterized by its coordinates (i, j), where $i \in \{1, 2, \ldots, I\}$ and $j \in \{1, 2, \ldots, J\}$. The decision variable $x_{i,j}(t)$ is defined as the percent of area treated in cell (i, j) in year t.

In order to incorporate different seed production rates for different age groups, we define age groups (classes) $k = 1, 2, 3, \ldots, n^+$, where each age group k defines a class of k year(s)-old species population, except that age group n^+ includes the n-year-old and older population. Therefore, for individuals that reach maturity at the age of n, where n can be any number depending on the species, transition population densities in cell (i, j) are formulated as

$$NP^k_{i,j}(t+1) = \delta \rho SB_{i,j}(t) \quad k = 1 \text{ and } \forall i, j, t \tag{1}$$

$$NP^k_{i,j}(t+1) = NA^{k-1}_{i,j}(t)(1 - \varphi_{k-1}) \quad k = 2, \ldots, n-1 \text{ and } \forall i, j, t \tag{2}$$

$$NP^k_{i,j}(t+1) = NA^{k-1}_{i,j}(t)(1 - \varphi_{k-1}) + NA^k_{i,j}(t)(1 - \varphi_k), \quad k = \mathrm{n}^+ \text{ and } \forall i, j, t \tag{3}$$

where δ is the seed germination rate, ρ is the survival rate of plants after becoming a seedling, $SB_{i,j}(t)$ is a function representing seed bank population at time t, φ_k is the loss rate of individuals when age class k grows into age class $k + 1$, $NA^k_{i,j}(t)$ is the population after treatment for the age class k at the beginning of time period t, and $NP^k_{i,j}(t+1)$ represents the potential population for age class k in cell (i, j) at the beginning of time period $t + 1$ before carrying capacity is considered.

Equation (1) gives the number of one-year-old individuals at the beginning of period $t + 1$ that have germinated from the seed bank in time period t and become seedlings. Equation (2) denotes the transition population levels of individuals that are $k = 2, \ldots, n - 1$ years old at the beginning of period $t + 1$ and were subject to individual losses at rate φ_{k-1} due to seasonal changes and ecological factors in period t. Equation (3) provides the number of n^+-year-old individuals at the beginning of period $t + 1$, which are $n - 1$ and n^+ years old and exposed to individual losses at rate φ_{n-1} and φ_{n^+}, respectively, in period t.

Here, we consider an invasive plant that disperses only through seeds. It is assumed that some of the seeds will be dispersing to eight adjacent cells, and some of them will remain within the cell. Define M^{ij} as the set of eight adjacent cells of a cell (i, j), where $M^{ij} = \{(i+1, j+1), (i+1, j), (i, j+1), (i-1, j-1), (i-1, j), (i, j-1), (i-1, j+1), (i+1, j-1)\}$.

We then formulate the seed dispersal to cell (i,j) from its surrounding eight neighbors $(h, w) \in M^{ij}$ as

$$SD_{i,j}(t) = \lambda \sum_{k=1}^{n} \sum_{(h,w) \in M^{ij}} S(k) NA^k_{h,w}(t) \quad \forall i, j, t \tag{4}$$

where λ is the proportion of seeds produced in neighboring cells that disperse to cell (i, j) in period t, $S(k)$ is the number of seeds produced by one individual of age class k, and $NA^k_{h,w}(t)$ is the number of the individuals of age class k in the surrounding cell $(h,w) \in M^{ij}$ following treatment. Equation (4) gives the total number of seeds dispersed from eight surrounding cells to cell (i, j).

The number of seeds remaining in cell (i, j) after dispersal is then given as

$$Seed_{i,j}(t) = \theta \sum_{k=1}^{n} NA^k_{i,j}(t) S(k), \quad \forall i, j, t \tag{5}$$

where $\theta = 1 - 8\lambda$ is the proportion of locally produced seeds that remain in cell (i, j). Equation (5) gives the total number of seeds produced in cell (i, j), after dispersal.

Journal : Medium 10530 | Dispatch : 9-4-2015 | Pages : 19
Article No. : 893 | LE | TYPESET
MS Code : BINV-D-14-00515 | CP | DISK

After seed production by each individual, seeds can germinate, experience mortality from pathogens or seed predators, or become dormant, thus forming a seed bank. Hence, the longevity (viability) rate of seeds, which is defined by the percentage of seeds in the seed bank that remain viable over time, and the germination rate are important factors that must be considered when modeling the seed bank population. Therefore, the number of seeds in the seed bank in cell (i, j) at time t, $SB_{i,j}(t)$ is formulated as

$$SB_{i,j}(t) = \sum_{s=0}^{t}\left((\gamma-\delta)^{t-s}\ \left(SD_{i,j}(s) + Seed_{i,j}(s)\right)\right) + SB_{i,j}(0)(\gamma-\delta)^{t} \quad \forall i, j, t \tag{6}$$

where γ and δ represent the longevity rate and germination rate of seeds in the seed bank, respectively. Equation (6) indicates that the seed bank population in cell (i,j) at time t includes seeds dispersing from the surrounding cells ($SD_{ij}(.)$), seeds that are produced but not germinated within the cell ($Seed_{i,j}(.)$), and the initial seed bank population ($SB_{ij}(0)$). Note that $SD_{ij}(s)$ and $Seed_{ij}(s)$ are given in Eqs. (4) and (5), respectively. Also note that in Eq. (6), the seed bank population has a compound increasing rate depending on the longevity and germination rate of the seeds, which decays as time passes.

Although invasive species commonly produce many offspring, natural boundaries, soil characteristics, and ecological factors constitute barriers for total population in a given cell so that the population cannot exceed the carrying capacity of cell (i, j), $K_{i,j}$, which is the maximum density (number of individuals) in cell (i, j) (for alternatives see Appendix S2). Therefore, the actual individual population before treatment, $NB^{k}_{i,j}(t)$, is formulated as

$$NB^{k}_{i,j}(t) = \min\left\{NP^{k}_{i,j}(t), K_{i,j}\right\}, \quad k = n^{+} \text{ and } \forall i, j, t \tag{7}$$

$$NB^{k}_{i,j}(t) = \begin{cases} 0 \ \textit{if}\ K_{i,j} - \sum\limits_{a=k+1}^{n^{+}} NB^{a}_{i,j}(t) \le 0, \\ \min\left\{\left(K_{i,j} - \sum\limits_{a=k+1}^{n^{+}} NB^{a}_{i,j}(t)\right), NP^{k}_{i,j}(t)\right\} \textit{otherwise} \end{cases}$$
$$k = 1 \ldots n^{+} - 1 \text{ and } \forall i, j, t \tag{8}$$

Equations (7) and (8) ensure that previously established plants occupy cell (i,j) before younger individuals do. If the cell population does not reach carrying capacity by the individuals of age class n^{+}, the second-oldest class adds to the population up to the carrying capacity. This cycle continues until the population reaches the maximum population level in each cell. In particular, Eq. (7) allows the model to give priority to the oldest age class n^{+} in a given cell (i,j). If the transition population of the oldest individuals in cell (i,j) is more than the carrying capacity, the before-treatment population of the oldest individuals will be set to the carrying capacity; otherwise, it will be set to their transition population. Once the oldest age class n^{+} is given priority, the model allows age class $n^{+} - 1$, $n^{+} - 2, \ldots, 1$ to occupy the remaining space from the age class n^{+}, respectively. The first part of Eq. (8) $\left(0 \text{ if } K_{i,j} - \sum\limits_{a=k+1}^{n^{+}} NB^{a}_{i,j}(t) \le 0\right)$ states that if the carrying capacity in cell (i, j) is reached by individuals at age class older than k, kth (and younger) age class will not be able to populate cell (i, j). The second part of the Eq. (8) indicates that the before-treatment population of the kth age class will be set to the minimum of the remaining space available or the transition population of the kth age class.

In the case of treatment, the before-treatment population is multiplied by the factor $\left(1 - \omega x_{i,j}(t)\right)$ where ω is the treatment efficacy, and $x_{i,j}(t) \in [0, 1]$ is a decision variable representing the percentage area treated in cell (i, j) in year t. Therefore, the population after treatment for age class k, $NA^{k}_{i,j}(t)$, is calculated by

$$NA^{k}_{i,j}(t) = NB^{k}_{i,j}(t)\left(1 - \omega x_{i,j}(t)\right) \quad \forall k, i, j, t \tag{9}$$

The treatment in each time period t is limited by available budget for treatment and labor. Therefore, the budget constraint becomes

$$\sum_{i=1}^{I}\sum_{j=1}^{J}\left(C_{i,j} + H_{i,j}\right)x_{i,j}(t) \le B(t) \quad \forall t \tag{10}$$

where $C_{i,j}$ is the treatment labor cost per cell (i, j), $H_{i,j}$ is the specific (e.g., herbicide) cost of treatment per cell (i, j), and $B(t)$ is the available budget for treatment and labor at time period t. Equation (10)

Journal : Medium 10530 | Dispatch : 9-4-2015 | Pages : 19
Article No. : 893 | LE | TYPESET
MS Code : BINV-D-14-00515 | CP | DISK

ensures that the total amount of a budget spent for treatments in a period t cannot exceed the available budget in period t.

The objective of the model is to minimize the total economic damages caused by the invasive species population in all cells and all periods of the planning horizon. The objective function is then formulated as

$$\text{Minimize } z = \sum_{i=1}^{I} \sum_{j=1}^{J} \sum_{t=1}^{T} D_{i,j}(t) \quad (11)$$

where $D_{i,j}(t)$ represents the damage as an economic loss due to invasion in cell (i, j) at the beginning of time t. The term $D_{i,j}(t)$ is given as

$$D_{i,j}(t) = E_{i,j}(t) \frac{\sum_{k=1}^{n} NA_{i,j}^{k}(t)}{K_{i,j}}, \quad \forall i, j, t \quad (12)$$

where $E_{i,j}(t)$ represents the economic value of cell (i,j). The total sum of individuals at different age classes represents the total population in cell (i,j) at the beginning of time period t. In Eq. (12), the loss of economic value in cell (i, j) is proportional to the ratio of the total population with respect to carrying capacity, $K_{i,j}$, in that cell.

Case study: control of sericea invasion in the Great Plains

Sericea is a drought-tolerant legume that can grow in a range of soil types, produces copious seeds, and has a long-lived seed bank (Ohlenbusch et al. 2007). Sericea was declared a noxious weed by the Kansas Department of Agriculture in 2000, has spread over 2,226,337 ha of the mid- to southern Great Plains (Duncan et al. 2004), and has led to \$29 million average annual forage loss in the Flint Hills region of Kansas (Fechter and Jones 2001). Furthermore, this legume replaces the native species in grasslands and threatens biodiversity in the Great Plains. Although herbicides can effectively eradicate established plants, populations can quickly recover from control strategies by germination from the seed bank. Given the biological characteristics of sericea and limited financial resources, determining the most effective long-term control strategy is difficult without the use of complex response models. Our bio-economic optimization model provides decision strategies regarding where and when limited funds can be best allocated for effective control of invasions by applying a restricted budget across a 15-year planning horizon.

The objective of the model is to minimize economic loss from haying and grazing due to sericea invasion. A gridded landscape is utilized to represent the spatially heterogeneous growth, spread, damage, and control costs. In this case study, we represent the initial invasion on a 10×10 landscape (40 ha), where each cell represents 0.4 ha of land. We examine responses using population maps reflecting three different frequency levels, representing the percentage of invaded areas of the gridded landscape—at 2 % (low), 40 % (medium), and 80 % (high)—and three different abundance rates defining species population in each cell—such as U[1–20] (low), U[21–200] (medium), and U[201–2000] (high), where U[a–b] denotes an integer number drawn uniformly from the interval [a, b] (Table 1). Therefore, nine different maps, each defined by a combination of three frequency and three abundance levels of the species, could be generated. However, for the sake of conciseness, the model is applied to the most representative five cases, which include extreme and average cases, and provide sufficient information regarding computational analysis: low frequency and low abundance (L–L), low frequency and high abundance (L–H), medium frequency and medium abundance (M–M), high frequency and low abundance (H–L), and high frequency and high abundance (H–H). Each case is a randomly generated initial population distribution, as shown in the first column of Fig. 2 (Maps a1–f1). Note that ten different maps are randomly generated for each of the five cases. Therefore, we utilize 50 maps and present the average results of ten maps for each case in each computational simulation (Figs. 1, 2, 3, 4, 5, 6).

Along with the initial population structure, we present model parameters with their symbols, units, and case study values (Table 1), in order to demonstrate the general behavior of the model. Sericea ramets generally start to produce seeds after two growing seasons, with the majority of ramets producing seed in year three. Using the information from Schutzenhofer and Knight (2007) and Woods et al. (2009), we estimate seed production as 45 and 900 per ramet for two- and three-year-old ramets, respectively. Therefore, we divide the sericea population into one-, two-, and three^{+}-year-old age classes in order to

Journal : Medium 10530 | Dispatch : 9-4-2015 | Pages : 19
Article No. : 893 | ☐ LE | ☐ TYPESET
MS Code : BINV-D-14-00515 | ☑ CP | ☑ DISK

Table 1 Initial population structure and parameters

Description	Frequency (%)	Category
Percentage of cells invaded in 10 × 10 landscape	2	Low frequency
	40	Medium frequency
	80	High frequency

Description	Abundance	Category
Initial population of sericea ramets in one cell	U[1–20]	Low abundance
	U[21–200]	Medium abundance
	U[201–2000]	High abundance

Model parameter	Symbol	Units	Case study values	References
Loss rate from age cluster k to $k + 1$	$\varphi(k)$	–	22, 9, 4** %	1
Number of seeds produced per ramet per age cluster k	$S(k)$	–	0, 45, 900	2
Percentage of seed dispersal	λ	–	0.01, 0.1*, 1 %	3
Percentage of remaining seeds	θ	–	99.92, *99.2*, 92 %	3
Longevity rate	γ	–	95 %	3
Germination rate	δ	Seedlings/seeds	6.8 %	4
Survival rate of seedlings	ρ	–	90 %	5
Carrying capacity	K_{ij}	Ramets/0.4 ha	1,936,000	4
Treatment efficacy of herbicides	ω	–	90, *95*, 99 %	6
Labor cost	C_{ij}	\$/0.4 ha	\$3.25	3
Herbicide cost	H_{ij}	\$/0.4 ha	\$10.50	6
Budget allotted to control sericea in year t	$B(t)$	\$	[0, 1400]	
Revenue from hay	–	\$/0.4 ha	\$306	7
Revenue from forage	–	\$/0.4 ha	\$81.71	7

1, Schutzenhofer et al. (2009); 2, Woods et al. (2009); 3, Expert opinion; 4, Houseman et al. (2014); 5, Houseman unpublished data; 6, Lance et al. (1997); 7, K-State (2012)

* Underlined parameter values that correspond to percentage of seed dispersal, percentage of remaining seeds, and treatment efficacy of the herbicide represent reasonable baseline parameter values, which are derived from the related literature and based on expert opinion. The values to the left and right of the italicized parameters are used for sensitivity analysis in order to analyze the behavior of the model in extreme cases

** Values separated by commas regarding "Loss rate from age cluster k to $k + 1$" and "Number of seeds produced per ramet per age cluster k" represent case study values for 1, 2 and 3^+ years old age classes

incorporate different plant mortality and seed production rates for each age class. Based on this model, one-year-old ramets become two-year-old ramets, and two-year-old ramets become three-year-old ramets with a loss rate of 22 and 9 %, respectively, while three-year-old and older ramets remain in the three$^+$ age class with a loss rate of 4 % each year. The loss rate decreases each year until a ramet reaches maturity because the mortality risk presumably decreases as plant size increases (Schutzenhofer and Knight 2007). Survival rate ρ is assumed to be 90 %, which is the percentage of seedlings that are able to survive after germination. The case study focuses on the economic impact of sericea invasion in grasslands found in the central Great Plains of North America. However, this application could be adjusted to different land types and competition against existing vegetation by reducing the survival rate of seedlings or increasing the loss rates of one-year old ramets based on the density of initial existing vegetation.

Although most sericea seeds disperse very near the maternal plant, some will disperse to surrounding areas by natural disturbances such as wind, animal, and human interaction (Houseman unpublished data). Therefore, seed dispersal from cell (i,j) to the surrounding eight cells is estimated by a dispersal

Journal : Medium 10530 | Dispatch : 9-4-2015 | Pages : 19
Article No. : 893 | ☐ LE | ☐ TYPESET
MS Code : BINV-D-14-00515 | ☑ CP | ☑ DISK

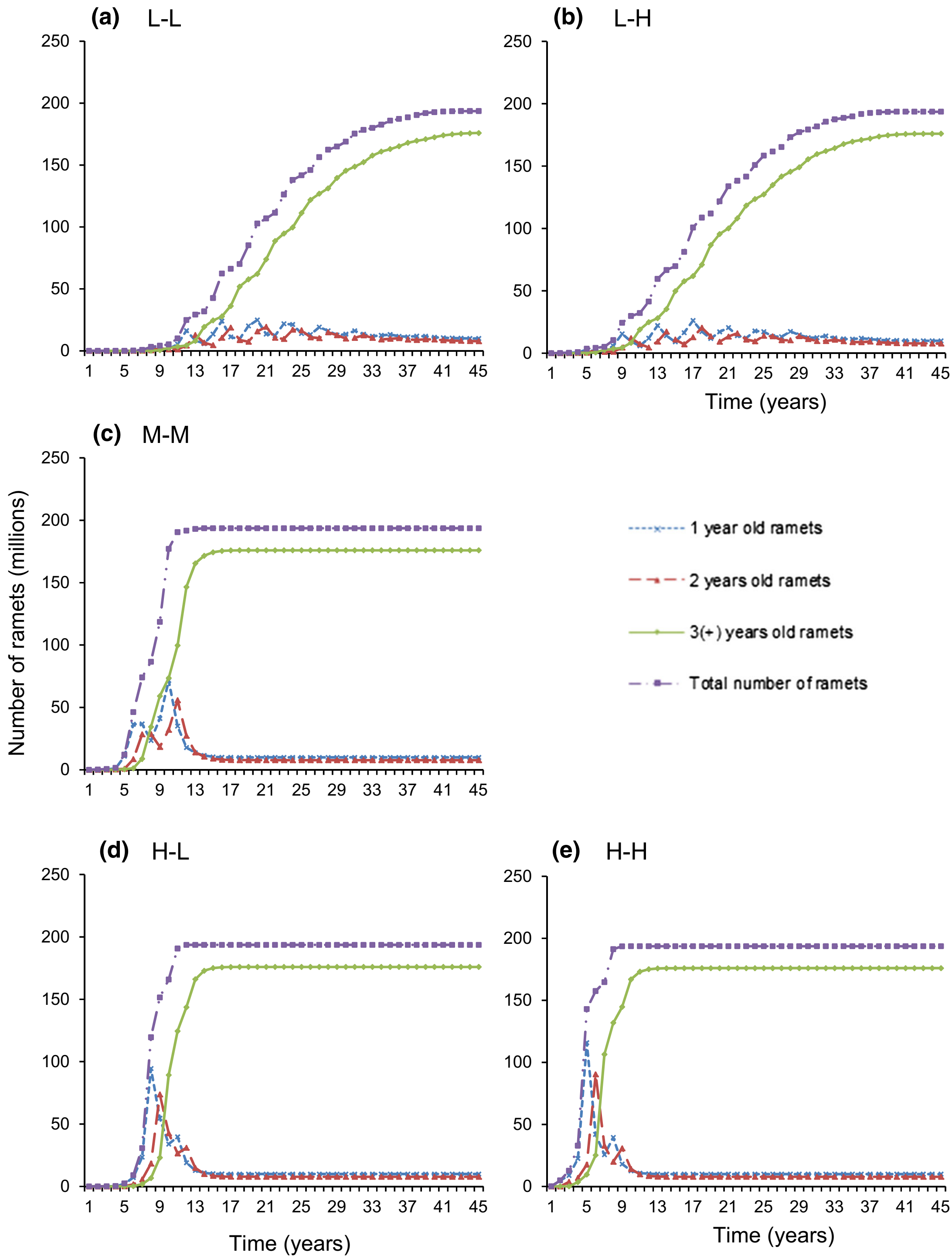

Fig. 1 Field-level invasion by sericea for three age classes over 45 years in the absence of control measures under initial conditions consisting of **a** low frequency and low abundance (L–L), **b** low frequency and high abundance (L–H), **c** medium frequency and medium abundance (M–M), **d** high frequency and low abundance (H–L), and **e** high frequency and high abundance (H–H)

Journal : Medium 10530 | Dispatch : 9-4-2015 | Pages : 19
Article No. : 893 | LE | TYPESET
MS Code : BINV-D-14-00515 | CP | DISK

constant $\lambda = 0.1$ % in the baseline scenario. We assume that there are no seeds in the seed bank at the beginning of year 1. Based on field experiments, the carrying capacity is set to 1,936,000 ramets per cell considering various conditions including competition with other vegetation (Houseman et al. 2014). We set a constant carrying capacity without differentiating among age clusters because field experiments show that most of the plants will be mature (at the 3^+-year-old cluster) when the carrying capacity is reached.

In our model, some proportion of sericea ramets will be eradicated from each cell, depending on the effectiveness of the herbicide treatment. The treatment efficacy is set to an average value of 95 % in the baseline scenario (Lance et al. 1997). Moreover, the treatment cost of each cell (i, j) depends on the labor and herbicide cost, which is estimated as \$3.25 (expert opinion) and \$10.50 (Lance et al. 1997), respectively. The objective function minimizes the total economic loss (damage) caused by sericea over all cells of the grid for 15 years. Sericea invasion significantly reduces the economic value from haying and grazing in the Great Plains. Assuming that the expected land use involves both haying and grazing equally, damage is computed as the average revenue from haying and grazing multiplied by the proportion of the total sericea population with respect to the carrying capacity.

Given the input data (Table 1), the proposed mathematical model is solved using "CONOPT," a solver for large-scale nonlinear optimization (NLP) problems, in AMPL (Fourer et al. 2003) through the Internet-based NEOS (Network-Enabled Optimization System) Dell PowerEdge R420 server with a 2× Intel Xeon X5660 at 2.8 GHz (12 cores total) CPU and 64.0 GB memory (Czyzyk et al. 1998). The algorithm used in CONOPT is based on the Generalized Reduced Gradient (GRG) algorithm and preferable for models with high degrees of nonlinearity and also where feasibility is difficult to reach (Drud 1985). In this paper, due to the complexity of the problem, we employ a rolling horizon approach, where the NLP model is solved for each period, and then the resulting population density at each cell is used as an initial condition for the next period's problem.

In order to analyze the model's response and behavior in extreme cases, we run the model under different values for some uncertain parameters such as budget, treatment effectiveness, and dispersal, considering their potential range. For example, in our model, the expected treatment effectiveness is set at 95 %. However, based on the data, we have an upper and lower bound defining the treatment effectiveness range. Therefore, we find the solution for the upper and lower bounds and the mean value of possible treatment effectiveness one at a time by fixing all the remaining parameters to their expected values. Likewise, the dispersal rate can be affected by wind, animal, and human activity. Therefore, we solve the model for the extreme values of the dispersal rate to determine the impact of dispersal under these situations.

Results

In this section, we present the results of five different computational simulations and sensitivity analyses. By solving the model with CONOPT, the optimal results for a \$0 budget level for all cases were achieved in less than 550 CPU seconds, and the optimal results for all other budget levels for all cases were achieved in less than 150 CPU seconds.

Part a: Growth behavior of different age groups over 45 years

In the first computational simulation, we analyze yearly population changes of sericea without herbicide treatment by observing the growth of one-, two-, and three$^+$-year-old ramets on a 10 × 10 landscape for five different initial populations with different frequencies and abundances for 45 years (Fig. 1).

In the M–M, H–L, and H–H cases (Fig. 1c–e), the growth of sericea follows a bi-logistic growth form, where there are two distinct phases, each with a logistic pattern as proposed by Meyer (1994). On the other hand, in the L–L and L–H cases (Fig. 1a, b), the growth of sericea follows a multi-logistic growth (Meyer et al. 1999) with multiple, sequential and overlapping phases of simple logistic form (see Appendix S1). Here, multi-logistic growth represents a growth function that includes serial, overlapping logistic phases, in which a successive section of the multi-logistic curve shows a slowing rate of growth as the population approaches the carrying capacity and finally saturate when carrying capacity is reached (Fig. 1a, b). For example, in Fig. 1a (L–L case), a

Journal : Medium 10530 | Dispatch : 9-4-2015 | Pages : 19
Article No. : 893 | ☐ LE | ☐ TYPESET
MS Code : BINV-D-14-00515 | ☑ CP | ☑ DISK

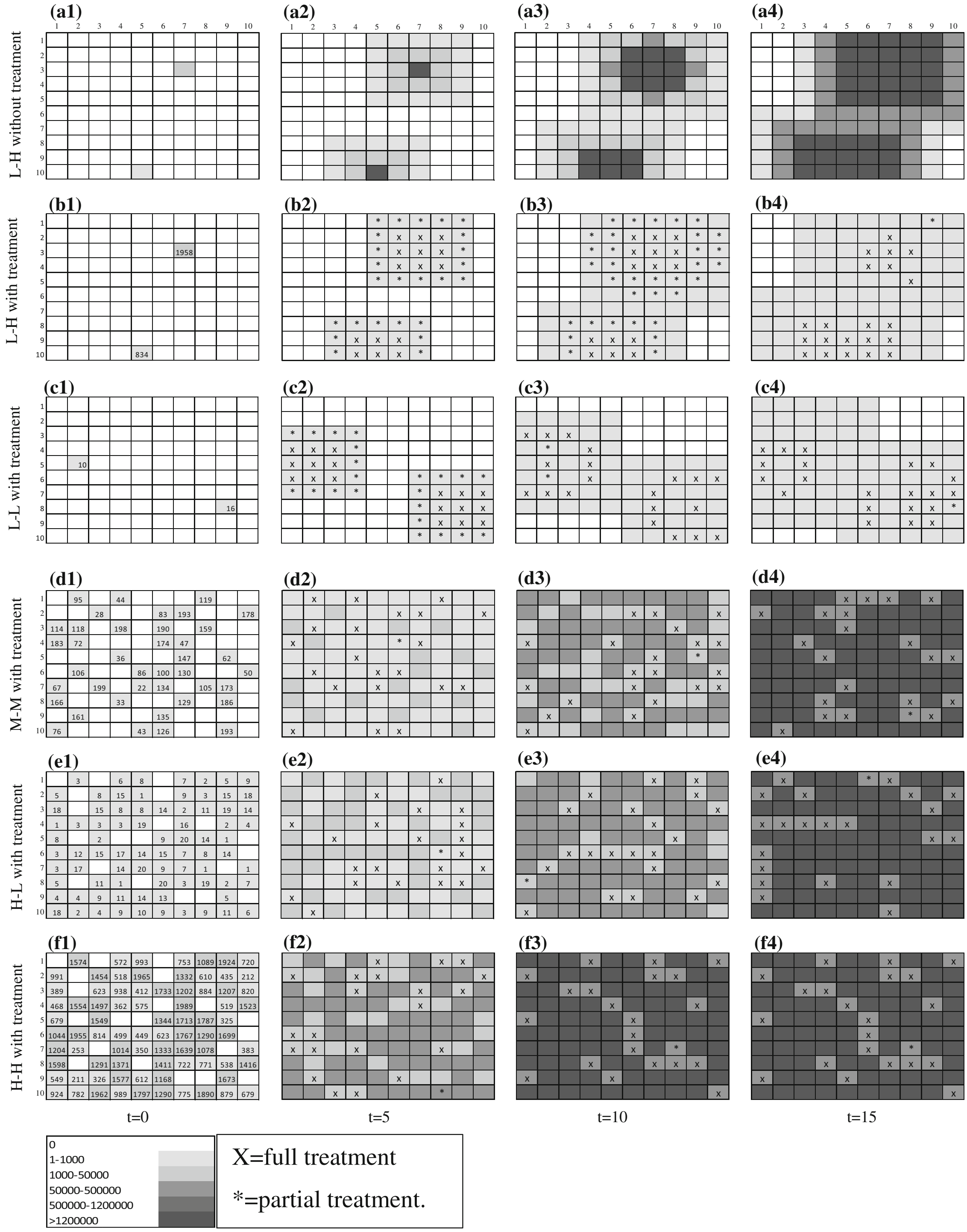

Fig. 2 Maps of plant spread with and without treatment, and treatment locations. The *rows* **a**–**f** represent different initial frequency and abundance scenarios (L–H: low frequency–high abundance, L–L: low frequency–high abundance, M–M: medium frequency–medium abundance, H–H: high frequency–high abundance) and the population abundance either with or without treatment while the columns represent different time steps in years (t)

Journal : **Medium 10530** Dispatch : **9-4-2015** Pages : **19**
Article No. : **893** ☐ LE ☐ TYPESET
MS Code : **BINV-D-14-00515** ☑ CP ☑ DISK

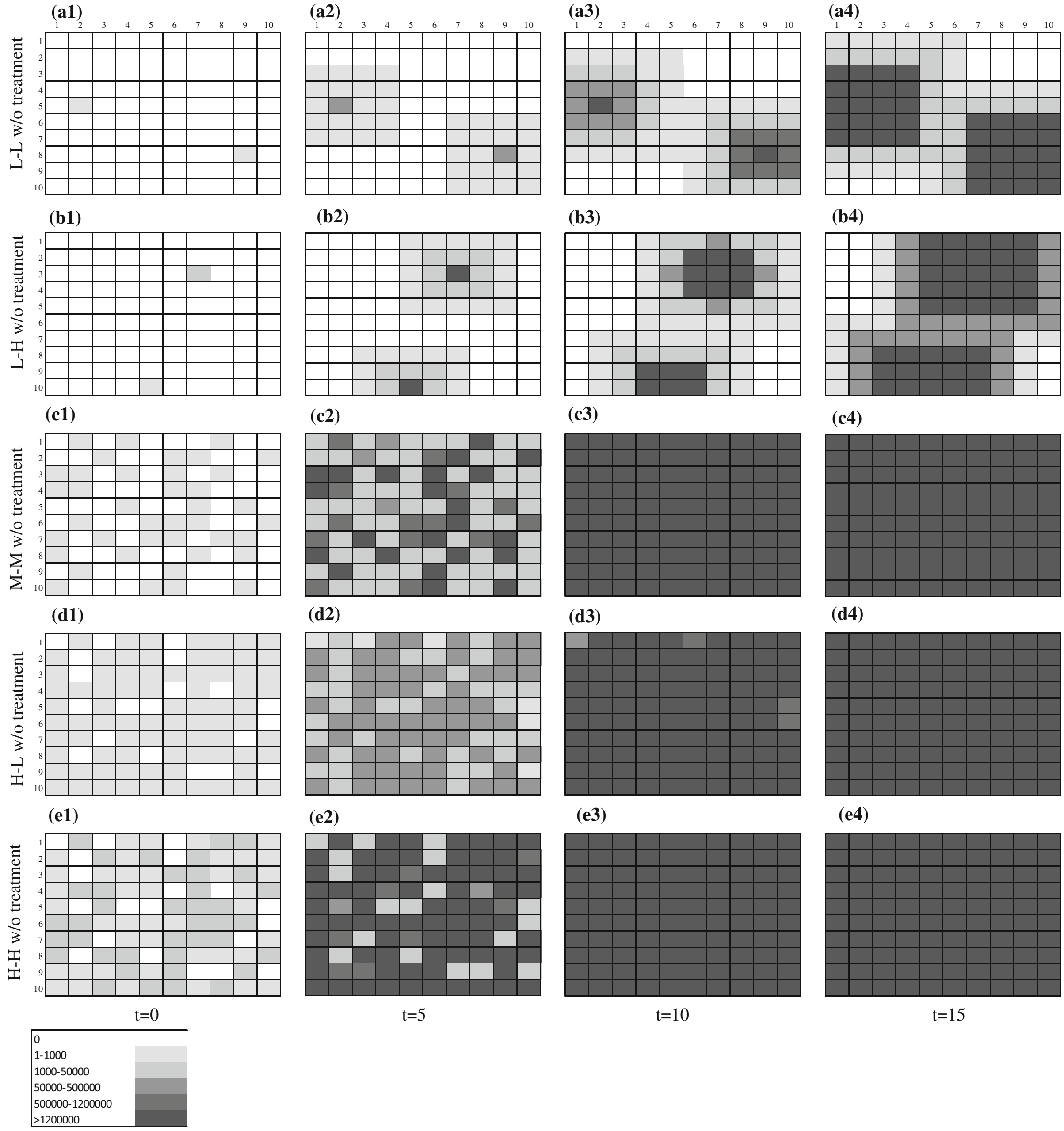

Fig. 3 Maps of plant spread without treatment. The *rows* **a**–**e** represent different initial frequency and abundance scenarios (L–L: low frequency–high abundance, L–H: low frequency–high abundance, M–M: medium frequency–medium abundance, H–H: high frequency–high abundance) and the population abundance without treatment while the *columns* represent different time steps in years (t)

logistic growth function or a growth phase is observed from year 9 to year 14, while another logistic function occurs from year 13 until year 18. Over a few decades, the multiple logistic growth functions dampen and show an asymptotic behavior. Note that we observe only two logistic growth phases in the M–M, H–L, and H–H cases, because carrying capacity is reached in these cases faster than the L–L and L–H cases.

In Fig. 1, we also observe that in all cases, the population of one- and two-year-old ramets is oscillating

Journal : **Medium 10530**	Dispatch : **9-4-2015**	Pages : **19**
Article No. : **893**	□ LE	□ TYPESET
MS Code : **BINV-D-14-00515**	✔ CP	✔ DISK

in time due to higher loss rates than older stages and limitations imposed by the carrying capacity, whereas the population of three^{+}-year-old ramets is increasing monotonically each year until carrying capacity is reached. This observed pattern of sericea growth can explain the multi (bi)-logistic behavior on a landscape with variation in the initial frequency and density of invasion among cells. Because reproduction is high and dispersal distance is limited, cells that have sericea plants quickly reach carrying capacity, while establishment into unoccupied cells is relatively slow. At the entire landscape scale, this translates into a multi-logistic rather than a smooth logistic pattern. Our computational tests also confirm that spatial progression of the sericea population growth has the largest impact on the observed oscillations during logistic growth. This response is also consistent with the responses of the different age classes. For example, at low-frequency invasion, the contribution of the first two age groups is high until newly occupied cells reach carrying capacity, at which point the three^{+}-year-old age class becomes dominant, and the one- and two-year-old age classes start to diminish. Because new cells on the landscape are occupied, a spike in the one- and two-year-old age classes occurs followed by a shift to the three^{+}-year-old age class forming a logistic growth phase. For landscapes with moderate- to high-frequency invasion (Fig. 1c, e), this spike in one- and two-year-old age classes is much higher, and we observe fewer growth phases than for landscapes with low-frequency invasion.

Part b: Plant spread with and without treatment, and treatment locations

In Fig. 2, maps a1–a4 represent the plant spread without treatment for L–H at $t = 0$, 5, 10, and 15 respectively, while maps b1–f4 represent initial population distribution at $t = 0$ and treatment locations at t = 5, 10, and 15 for L–H, L–L, M–M, H–L, and H–H, respectively, for a \$300 budget allocation each year. In Fig. 3, maps a1–f4 represent the initial population distribution at $t = 0$ and the plant spread without treatment at $t = 5$, 10, and 15 for the L–L, L–H, M–M, H–L, and H–H cases, respectively.

Maps b1–b4 in Fig. 2 suggest that in the L–H case, applying herbicide treatment in more cells with full and partial treatment results in less economic damage than applying treatment to fewer cells with only full treatment. On the other hand, applying full treatment to fewer cells with the highest invasion is the preferable method as the frequency and abundance of the invasion increases. Results show that full and partial treatment should both be considered as a treatment strategy in the early years of L–L and L–H cases, in order to decrease the yearly economic loss. It is clearly seen from the maps of L–H cases (with and without treatment) that, although we apply treatment every year, the spread of sericea is inevitable unless 100 % of the ramets with seed production capability are eradicated. Any of the invaded cells is a potential treatment area, depending on budget availability.

Due to the seed bank, which is explicitly considered in the model, plant regeneration will take place every year as long as seeds remain viable in the soil. Results suggest that the treatment locations change over time for each different abundance and frequency level cases (Figs. 2, 3). For many cases, treatment is applied to locations with the highest invasion in an effort to optimally allocate a limited budget. However, closely looking at these figures, (e.g., c3 of Fig. 2 (with treatment) and a3 of Fig. 3 (without treatment)), the optimal solution does not always choose to treat the largest patches first; instead, in this case (in year 10), it follows a strategy to treat locations that surrounds the heavily invaded location. This strategy might be due to an effort of the model to confine invaded locations instead of treating them. This result implies that providing general recommendations and simple rule-of-thumb strategies may not be optimal for all cases.

Maps f3 and f4 of Fig. 2 show that treated cells are the same in $t = 10$ and $t = 15$. This occurs because the entire landscape in H–L and H–H cases reach carrying capacity earlier compared to L–L, L–H, and M–M (Figs. 2, 3). Once a cell reaches carrying capacity in H–L and H–H cases at any time point, sericea quickly recovers from herbicide treatment, and carrying capacity is reached again in the following year due to the rapid growth from seed bank. The same cells are treated every year after the tenth year in the H–H case, since changing the location of the treatment does not change the overall damage.

Part c: Impact of treatment efficacy on economic damages

Given the patterns of population growth without control measures, we examine the budget necessary to control invader growth. Figure 4 illustrates the tradeoff between the cost of control measures and

Journal : Medium 10530 | Dispatch : 9-4-2015 | Pages : 19
Article No. : 893 | LE | TYPESET
MS Code : BINV-D-14-00515 | CP | DISK

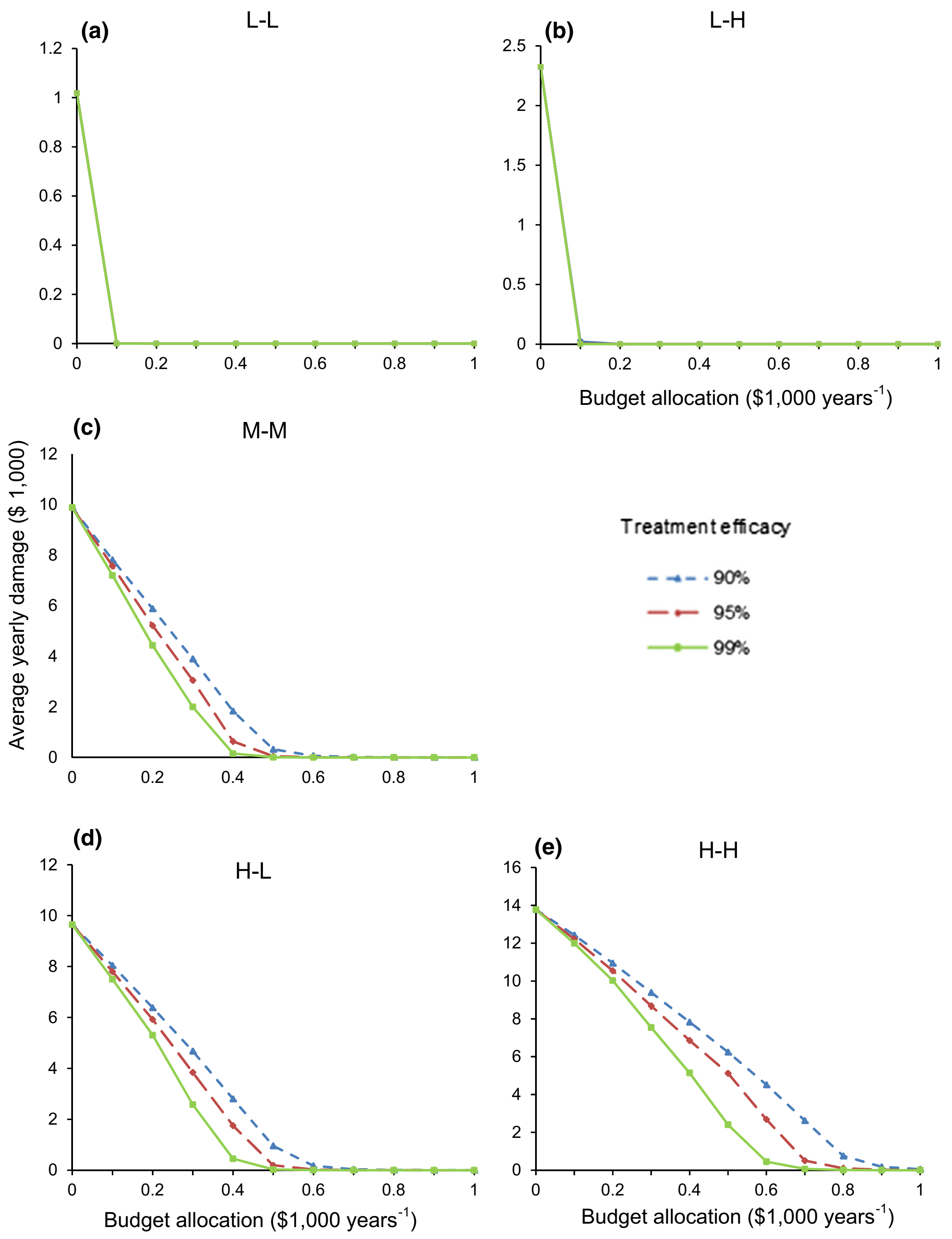

Fig. 4 Tradeoff between average yearly damages and budget allocation for different treatment efficacies over 15 years under initial conditions consisting of **a** low frequency and low abundance (L–L), **b** low frequency and high abundance (L–H), **c** medium frequency and medium abundance (M–M), **d** high frequency and low abundance (H–L), and **e** high frequency and high abundance (H–H). Values are non-zero near/at high values on the x-axis. *Note* differences in y-axis scale

Journal : **Medium 10530**	Dispatch : **9-4-2015**	Pages : **19**
Article No. : **893**	☐ LE	☐ TYPESET
MS Code : **BINV-D-14-00515**	☑ CP	☑ DISK

economic damage. Because the effectiveness of the treatment is uncertain due to year-to-year variation or the care with which herbicide is applied, we perform sensitivity analysis on different values of the treatment efficacy (90, 95, and 99 %) to analyze their impact on the yearly economic damage for different budget levels over 15 years (Fig. 4).

While a budget level of \$0.1 thousand is sufficient for the L–L and L–H cases (Figs. 4a, b), \$1 thousand, \$0.8 thousand, and \$0.6 thousand are required to completely eradicate the sericea population for 90, 95, and 99 % treatment efficacies, respectively, in the M–M case (Fig. 4c). The necessary budget increases to \$0.7 thousand for the 99 % treatment efficacy in the H–L case (Fig. 4d).

In the H–H case (Fig. 4e), sericea is eradicated with a budget allocation of \$1 thousand for a 99 % treatment efficacy but the necessary budget for eradication increases to \$1.3 thousand for a 95 % treatment efficacy. Here, a budget allocation of \$1 thousand for a 90 % treatment efficacy will lead to a damage level less than \$0.05 thousand but is not sufficient to completely eradicate the sericea population due to the widespread seed bank and the remaining few three^{+}-year-old ramets, which potentially generate an enormous amount of seeds that will add to the population in the following years.

Part d: Impact of dispersal rate on economic damages

Since the dispersal rate is potentially sensitive to variation in wind, animal, and human activity, we also perform sensitivity analysis on the impact of different spread rates (0.01, 0.1, and 1 %) on the yearly damage for different budget levels over 15 years. For each of these dispersal scenarios, the control costs (yearly budget on x-axis in Fig. 5) and the resulting economic damage are inversely related. When the dispersal rate level is increased from 0.1 to 1 %, the increase in the average yearly damage is equal to \$1.15 thousand for the L–L case, and \$0.41 thousand for the H–L case under no treatment (budget allocation = 0 on x-axis in Fig. 5). Furthermore, although the average yearly damage in the H–H case is more than the average yearly damage in the M–M case for all budget allocations, the impact of dispersal rates on the average yearly damage is more apparent in the M–M case. This occurs because seeds are more likely to spread to already-invaded cells in the H–H case than the M–M case, and the former is closer to the carrying capacity than the latter.

Part e: Impact of different treatment strategies on economic damages

We also examine the impact of three different treatment frequency strategies—every year (1-year), every 2 years (2-year), and every 3 years (3-year)—on the average yearly and total (cumulative) damages over 15 years (Fig. 6). Computational tests are conducted by equally allocating a total treatment budget of \$4.5 thousand for every year (\$0.3 thousand), every 2 years (\$0.56 thousand), and every 3 years (\$0.9 thousand) of the 15-year period, starting with treatment from the beginning of year 1.

Without treatment, the total damage increases from \$15.2 thousand to \$206.6 thousand by year 15, and all strategies reduce damage considerably, compared to no treatment in all cases (Fig. 6). In the L–L and L–H cases, the 1-year and 2-year strategies are the two best options, while the 3-year treatment strategy results in higher yearly and total damages (Fig. 6a, b). On the other hand, for the M–M case, the 2-year treatment strategy is more beneficial than the 1-year treatment (Fig. 6c). Here, less frequent control measures allow more of the population to be treated than the 1-year approach, and—because the recovery of the invader in a cell requires at least 2 years—the benefit of treating larger areas less frequently exceeds that of smaller areas treated more frequently. In other words, the immediate and higher reduction in total population that is the result of using the 2-year treatment approach is more beneficial than the 1-year approach, even though the economic damage as a result of the 2-year strategy exceeds the economic damage of the 3-year strategy in some years.

Results for the H–L and H–H cases suggest that the 3-year strategy will result in the lowest total costs over a 15-year period (Fig. 6d, e). The sericea population reaches carrying capacity earlier in the H–H case, compared to the other four cases, due to its high initial abundance. After the carrying capacity is reached, the \$0.9 thousand budget allocation compensates for damage in the previous years in the 3-year treatment strategy and thus causes less total damage at the end of year 15. On the other hand, the 1-year treatment results in more consistent damage levels than the 2-year and 3-year treatment strategies, which have substantial year-to-year variation in damages.

Journal : Medium 10530 | Dispatch : 9-4-2015 | Pages : 19
Article No. : 893 | ☐ LE | ☐ TYPESET
MS Code : BINV-D-14-00515 | ☑ CP | ☑ DISK

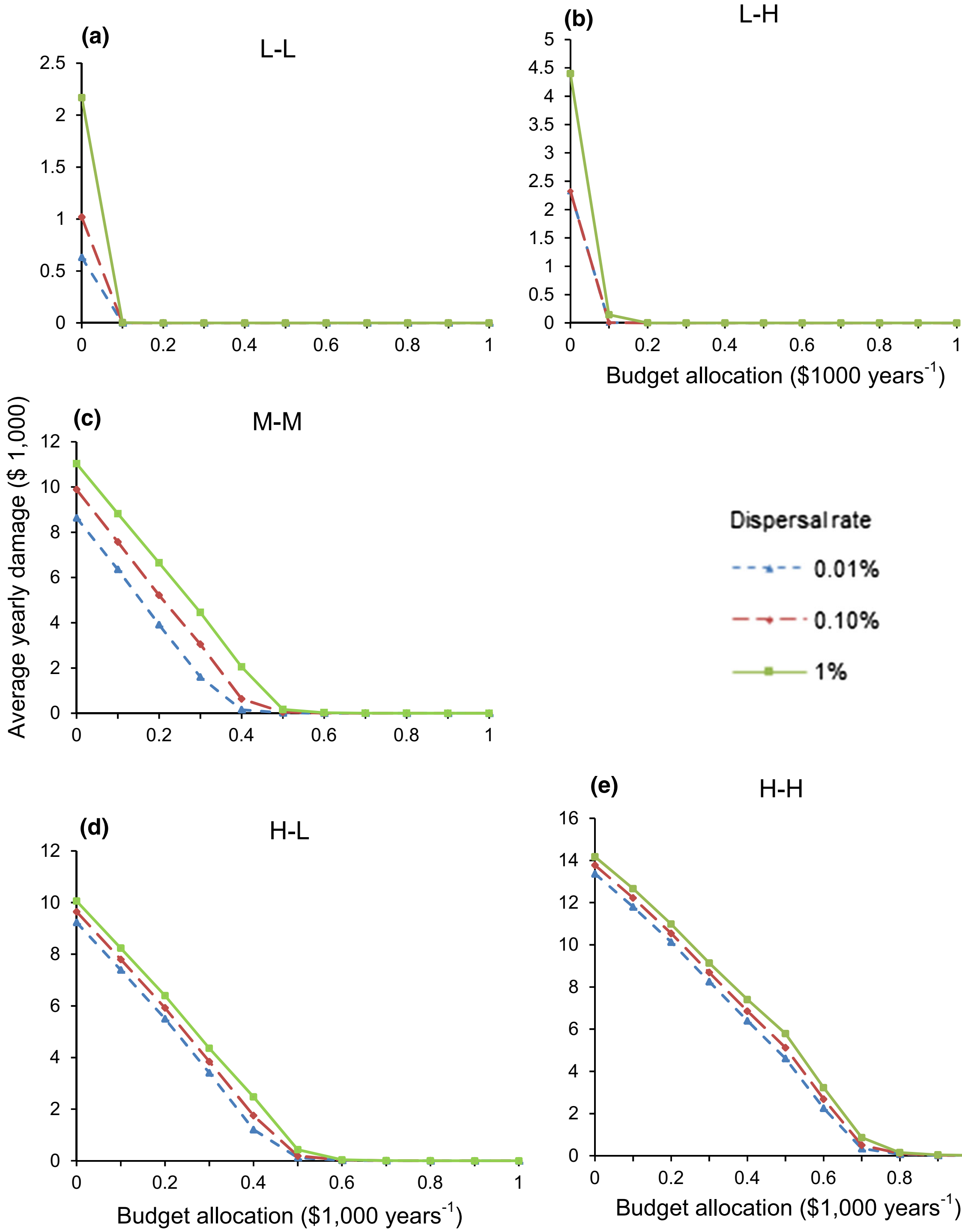

Fig. 5 Tradeoff between average yearly damages and budget allocation for different dispersal rates over 15 years under initial conditions consisting of **a** low frequency and low abundance (L–L), **b** low frequency and high abundance (L–H), **c** medium frequency and medium abundance (M–M), **d** high frequency and low abundance (H–L), and **e** high frequency and high abundance (H–H). Values are non-zero near/at high values on x-axis. *Note* differences in y-axis scale

Journal : **Medium 10530** Dispatch : **9-4-2015** Pages : **19**
Article No. : **893** ☐ LE ☐ TYPESET
MS Code : **BINV-D-14-00515** ☑ CP ☑ DISK

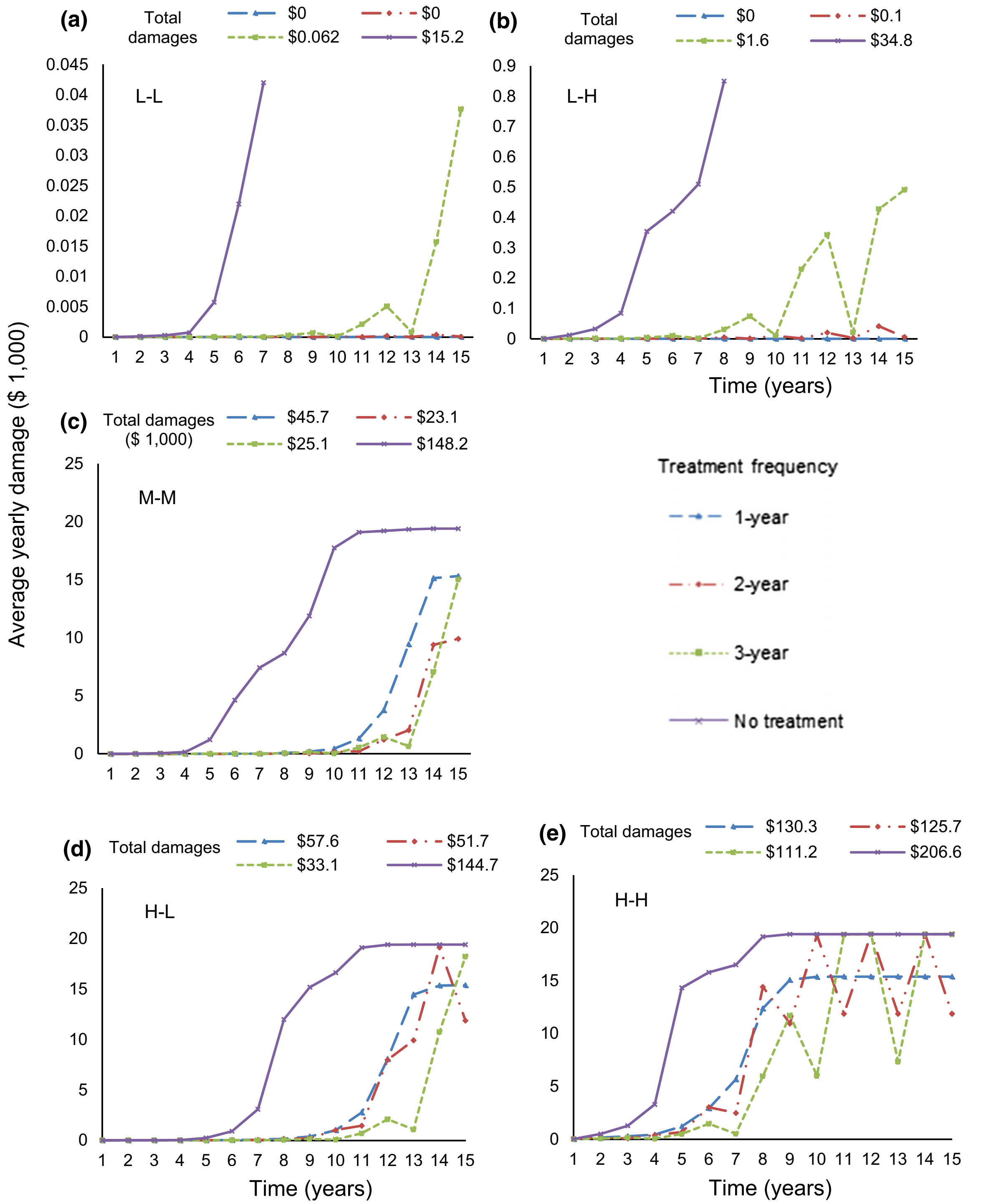

Fig. 6 Impact of different treatment frequency strategies on average yearly damage (presented on y-axis) and total (cumulative) damage (given above each subfigure) over 15 years under initial conditions consisting of **a** low frequency and low abundance (L–L), **b** low frequency and high abundance (L–H), **c** medium frequency and medium abundance (M–M), **d** high frequency and low abundance (H–L), and **e** high frequency and high abundance (H–H). *Note* differences in y-axis scale

Journal : **Medium 10530** Dispatch : **9-4-2015** Pages : **19**
Article No. : **893** ☐ LE ☐ TYPESET
MS Code : **BINV-D-14-00515** ✔ CP ✔ DISK

Discussion

We present a novel spatio-temporal dynamic model, which integrates biological models into a decision theory framework, while incorporating seed bank and dispersal, different age classes, growth rates, treatment costs, budget, and relevant economic loss. Unlike previous spatial–temporal methods (for a detailed discussion of these methods, see, e.g., Billionnet 2013), here the growth of the invasive population within each cell is modeled using the seed bank and influenced by the invasion state of neighboring cells, while the population is divided into classes of different age groups in order to reflect different seed production and loss rates of each age group into the model. Numerical results provide insights into biological growth and spread behavior of the species, in addition to strategies addressing relevant management questions.

The first key result is that the population growth response of sericea is more complex than simple logistic growth. In fact, the population follows a multi (bi)-logistic growth form, where there are multiple (two) distinct phases, each with a logistic pattern. Our results support Meyer's contention (1994) that the bi-logistic is useful in representing the growth of many systems that contain complex growth processes that are not well modeled by the simple logistic function. Here, we observe logistic phases of growth where in the first half of each phase, the first two age groups are dominant, and in the second half, the three^{+}-year-old age class becomes dominant, until carrying capacity is reached. Computational simulations show that the multi-logistic behavior could only be observed in a spatio-temporal model as proposed in this paper. The observed oscillations could be explained by the fast reproduction behavior of sericea, which allows it to reach the local carrying capacity quickly and then to start with a new establishment in surrounding newly arrived locations. The local growth of the species progresses spatially over time, and thus logistic growth phases are repeated until the entire landscape is invaded.

According to Cook (1965), although not typically examined, logistic growth of a population may undergo oscillations of one type or another, for many reasons including frequency related to age structure and time-lag effects. Introduced species commonly exhibit a lag-phase in which the non-native species remains at low abundance for an extended time before increasing exponentially (Aikio et al. 2010). Several proposed hypotheses suggest that this pattern results from genotypic, demographic, or extrinsic factors (Pysek and Hulme 2005). The multi (bi)-logistic response pattern exhibited by our model suggests that demographic factors may explain short-term lag-patterns and, when coupled with variation in extrinsic factors, may contribute to longer-term lag patterns. Such insight would not be possible with more simplistic models that ignore the biological detail included in our model and is likely to be relevant to other species with high seed production and persistent seed banks. Furthermore, the multi (bi)-logistic population growth pattern suggests that the timing of control measures may have stronger or weaker effects on the invader, depending on when treatment is applied.

It is interesting to note that although multiple logistic behavior is observed in many complex systems such as social diffusion and social change (Fokas 2007) and forecasting of technology change and short product lifecycles (Kucharavy and De Guio 2011; Trappey and Wu 2008), to our knowledge, this has never been shown before in an ecological context, either empirically or computationally. The empirical and theoretical community should consider when such variation (multi-logistic) might be important for invasive species control. For example, under what conditions is it important to model multi-logistic rather than logistic population growth when attempting to develop effective control strategies? Such questions are particularly relevant when searching for optimal solutions constrained by economic resources—as we attempt to do in this paper.

Second, given a target goal, the model addresses efficient management strategies regarding the following: (1) how large the allocated yearly budget needs to be, (2) the size of the infestation and where treatments should be targeted, and (3) how often treatments should be applied to be effective. In this paper, computational results demonstrate growth responses for three age classes under no-treatment, plant spread and treatment locations, tradeoffs between damage and budget levels, and the minimum required resources that must be allotted to alleviate the spread of sericea under various treatment and management scenarios.

Third, we perform sensitivity analysis with respect to treatment efficacy and seed dispersal parameters to analyze the impact of uncertainty on the model outputs and observe the model behavior for extreme scenarios.

Journal : Medium 10530 | Dispatch : 9-4-2015 | Pages : 19
Article No. : 893 | ☐ LE | ☐ TYPESET
MS Code : BINV-D-14-00515 | ✔ CP | ✔ DISK

Not surprisingly, the higher the treatment efficacy, the lower the damage levels, but interestingly, the impact of different treatment efficacies becomes clearer as the frequency levels increase. Such analyses illustrate the potential tradeoffs between the cost of treatment and its effectiveness for different initial population conditions. For example, by comparing the marginal (extra) cost with the marginal economic damage reduction benefit of using a more effective herbicide, managers decide whether to invest in the herbicide or not. Note that while we consider the most effective herbicide treatment and the corresponding cost in the sericea treatment case, the bio-economic model can also be extended to include various herbicide types or control strategies with their related costs. The results of this experiment also suggest that the average yearly damage increases as the dispersal rate increases for all budget levels and cases, but the dispersal rate has a higher impact for low-frequency initial population distributions than high-frequency initial invasions. Thus, a key component of invader control is the prevention of seed dispersal by reducing human and animal interaction.

Next, we evaluate three treatment timing strategies—1-year, 2-year, and 3-year—that could be used by managers, and we compare them with each other as well as the no-treatment option. Results suggest that effectiveness of the control strategy is highly dependent on initial population levels. With a limited budget, it is better to treat yearly if the initial population abundance and frequency is low, while it may be better to apply treatment every second or third year (with a higher per-treatment budget amount) when the frequency and abundance are high (Fig. 6).

In this paper, we address uncertainty by performing sensitivity analyses on different stochastic parameters such as budget, treatment efficacy, and dispersal rate. However, if the probability distributions of uncertain parameters are known or can be estimated, those parameters could be directly incorporated into the optimization model by defining them as random variables. The resulting stochastic nonlinear model could then be solved using stochastic optimization algorithms or heuristic approaches. Furthermore, for the application of the proposed model, we selected a spatial and temporal scale that was relevant to landscapes but was small enough to be tractable given the complexity of the model and current computational capacity. Future work could address issues of scale by employing advanced optimization approaches.

Our model could be utilized by a central planner who determines control actions with the minimum damage across multiple or private ownerships with respect to a shared budget and other constraints. Future research may include compensation of multiple owners under central decision-making or coordination of management among multiple decentralized decision-makers using game theoretic approaches (Büyüktahtakın et al. 2013; Forgó et al. 1999). Furthermore, if difficulties, including the quantification and formulation of ecological damages and preferences of stakeholders, are solved, this research could be extended to considering multiple objectives of different stakeholders including economic and ecological damages.

Our spatio-temporal approach can be extended to any species for which age structure is relevant such as fish, insects, mammals, and plants (see, e.g., Fazekas et al. 1997; Koji and Nakamura 2006; Tahvonen 2008; Shelton et al. 2012). For example, model Eqs. (1)–(3) that represent age-structured growth can be adjusted to model the growth of stage- or size-structured species, while seed generation and seed bank-based growth Eqs. (4)–(6) can be adjusted to model dormancy and various offspring generation, accumulation, and dispersal mechanisms. Furthermore, carrying capacity Eqs. (7), (8) can be adjusted to estimate the population abundances of different stage and size groups given carrying capacity limitations.

Results of the bio-economic optimization approach illustrate the potential for new optimization approaches that incorporate demographic detail and spatio-temporal realism for invasive species control into a single-decision framework. Furthermore, while the proposed model is specific enough to capture biological realism, it also has the potential to be generalized to a wide range of invasive plant and animal species under various management scenarios in order to identify the most efficient control strategy for managing invasive species over large, heterogeneous landscapes and long time periods.

Acknowledgments We gratefully acknowledge the support of the National Science Foundation under Grant No. EPS-0903806, the state of Kansas through the Kansas Board of Regents, and the Strategic Engineering Research Fellowship (SERF) of the College of Engineering at Wichita State University. We also thank two anonymous referees and the associate editor whose remarks helped to improve the clarity of our exposition.

Journal : Medium 10530 | Dispatch : 9-4-2015 | Pages : 19
Article No. : 893 | ☐ LE | ☐ TYPESET
MS Code : BINV-D-14-00515 | ☑ CP | ☑ DISK

References

Aikio S, Duncan RP, Hulme PE (2010) Lag-phases in alien plant invasions: separating the facts from the artifacts. Oikos 119(2):370–378

Albers HJ, Fischer C, Sanchirico JN (2010) Invasive species management in a spatially heterogeneous world: effects of uniform policies. Resour Energy Econ 32:483–499

Bhat MG, Huffaker RG, Lenhart SM (1993) Controlling forest damage by dispersive beaver populations: centralized optimal management strategy. Ecol Appl 3(3):518–530

Billionnet A (2013) Mathematical optimization ideas for biodiversity conservation. Eur J Oper Res 231:514–534

Blackwood J, Hastings A, Costello C (2010) Cost-effective management of invasive species using linear-quadratic control. Ecol Econ 69:519–527

Büyüktahtakın İE, Zhuo F, George F, Ferenc S, Olsson A (2011) A dynamic model of controlling invasive species. Comput Math Appl 62:3326–3333

Büyüktahtakın İE, Feng Z, Frisvold G, Szidarovszky F (2013) Invasive species control based on a cooperative game. Appl Math 4(10):54

Caswell H (2001) Matrix population models: construction, analysis, and interpretation, 2nd edn. Sinauer Associates, Sunderland

Clark C (1990) Mathematical bioeconomics: the optimal management of renewable resources, 2nd edn. Wiley, New York

Cook LH (1965) Oscillation in the simple logistic growth model. Nature 207:316

Czyzyk J, Mesnier M, Moré J (1998) The NEOS server. IEEE J Comput Sci Eng 5(3):68–75

Drud A (1985) CONOPT: a GRG code for large sparse dynamic nonlinear optimization problems. Math Program 31(2): 153–191

Duncan CA, Jachetta JJ, Brown ML, Carrithers VF, Clark JK, DiTomaso JM et al (2004) Assessing the economic, environmental, and societal losses from invasive plants on rangeland and wildlands. Weed Technol 18:1411–1416

Epanchin-Niell R, Hastings A (2010) Controlling established invaders: integrating economics and spread dynamics to determine optimal management. Ecol Lett 13(4):528–541

Epanchin-Niell RS, Wilen J (2012) Optimal spatial control of biological invasions. J Environ Econ Manag 63(2):260–270

Fazekas J, Kadar F, Sarospataki M, Lovei GL (1997) Seasonal activity age structure and egg production of the ground beetle *Anisodactylus signatus* (Coleoptera: Carabidae) in Hungary. Eur J Entomol 94:473–484

Fokas N (2007) Growth functions, social diffusion, and social change. Rev Sociol 13(1):5–30

Forgó F, Szép J, Szidarovszky F (1999) Introduction to the theory of games. Concepts, methods, applications. Kluwer, Dordrecht

Fechter RH, Jones R (2001) Estimated economic impacts of the invasive plant sericea lespedeza on Kansas grazing lands. J Agric Appl Econ 33:630

Fourer R, Gay DM, Kernighan BW (2003) AMPL: a modeling language for mathematical programming, Duxbury Press, Brooks/Cole-Thomson Publishing Company, Pacific Grove, CA

Getz WM, Haight RG (1989) Population harvesting: Demographic models of fish, forest and animal resources Monographs in Population Biology, vol 27. Princeton University Press, Princeton

Gurevitch J, Fox GA et al (2011) Emergent insights from the synthesis of conceptual frameworks for biological invasions. Ecol Lett 14(4):407–418

Hof J (1998) Optimizing spatial and dynamic population-based control strategies for invading forest pests. Nat Resour Model 11:197–216

Hof J, Bevers M (2002) Spatial optimization in ecological applications. Columbia University Press, New York

Houseman G, Foster B, Brassil CE (2014) Propagule pressure-invasibility relationships: testing the influence of soil fertility and disturbance with *Lespedeza cuneata*. Oecologia 174(2):511–520

Kaiser BA, Burnett KM (2010) Spatial economic analysis of early detection and rapid response strategies for an invasive species. Resour Energy Econ 32:566–585

Kansas State University (2012) 2012 Chemical weed control, SRP1063. http://www.atchison.ksu.edu/doc39521.ashx. Accessed 19 Jan 2014

Koji S, Nakamura K (2006) Seasonal fluctuation, age structure, and annual changes in a population of *Cassida rubiginosa* (Coleoptera: Chrysomelidae) in a natural habitat. Ann Entomol Soc Am 99:292–299

Kovacs KF, Haight RG, Mercader RJ, McCullough DG (2014) A bioeconomic analysis of an emerald ash borer invasion of an urban forest with multiple jurisdictions. Resour Energy Econ 36:270–289

Kucharavy D, De Guio R (2011) Logistic substitution model and technological forecasting. Procedia Eng 9:402–416

Lance TV, Terrence GB, Stritzke J (1997) Ecology and management of *Sericea Lespedeza*. http://pods.dasnr.okstate.edu/docushare/dsweb/Get/Rendition-7591/PSS-2874web+color.pdf. Accessed 19 Jan 2014

Leslie PH (1945) The use of matrices in certain population mathematics. Biometrika 33(3):183–212

Meyer PS (1994) Bi-logistic growth. Technol Forecast Soc Change 47:89–102

Meyer PS, Yung JW, Ausubel JH (1999) A Primer on logistic growth and substitution: the mathematics of the Loglet lab softwar. Technol Forecast Soc Change 61(3):247–271

Ohlenbusch DP, Bidwell T, Fick H, Scott W, Clubine S, Coffin M et al (2007) *Sericea Lespedeza*: history, characteristics, and identification. Kansas State University Agricultural Experiment Station, Cooperative Extension Service, Manhattan

Olson LJ (2006) The economics of terrestrial invasive species: a review of the literature. Agric Resour Econ Rev 35(1): 178–194

Pysek P, Hulme PE (2005) Spatio-temporal dynamics of plant invasions: linking pattern to process. Ecoscience 12(3): 302–315

Schreiber SJ, Lloyd-Smith JO (2009) Invasion dynamics in spatially heterogeneous environments. Am Nat 174(4):490–505

Schutzenhofer MR, Knight TM (2007) Population-level effects of augmented herbivory on *Lespedeza cuneata*: implications for biological control. Ecol Appl 17(4):965–971

Journal : Medium 10530 | Dispatch : 9-4-2015 | Pages : 19
Article No. : 893 | □ LE | □ TYPESET
MS Code : BINV-D-14-00515 | ✔ CP | ✔ DISK

Schutzenhofer M, Valone T, Knight T (2009) Herbivory and population dynamics of invasive and native lespedeza. Oecologia 161(1):57–66

Shelton A, Munch S, Keith D, Mangel M (2012) Maternal age, fecundity, egg quality, and recruitment: linking stock structure to recruitment using an age-structured Ricker model. Can J Fish Aquat Sci 69:1631–1641

Stone R (1980) Sigmoids. Bull Appl Stat 7:59–119

Tahvonen O (2008) Harvesting age-structured populations as a biomass. Does it work? Nat Resour Model 21:525–550

Taylor C, Hastings A (2004) Finding optimal control strategies for an invasive grass using a density-structured model. J Appl Ecol 41:1049–1057

Trappey CV, Wu HY (2008) An evaluation of the time-varying extended logistic, simple logistic, and Gompertz models for forecasting short product lifecycles. Adv Eng Inform 22(4):421–430

With KA (2002) The landscape ecology of invasive spread. Conserv Biol 16(5):1192–1203

Woods MT, Hartnett CD, Ferguson JC (2009) High propagule production and reproductive fitness homeostasis contribute to the invasiveness of *Lespedeza cuneata* (Fabaceae). Biol Invasions 11(8):1913–1927

Wu J (2001) Optimal weed control under static and dynamic decision rules. Agric Econ 25(1):119–130

Journal : **Medium 10530**	Dispatch : **9-4-2015**	Pages : **19**
Article No. : **893**	☐ LE	☐ TYPESET
MS Code : **BINV-D-14-00515**	☑ CP	☑ DISK